Supplement of Atmos. Meas. Tech., 16, 1323–1341, 2023
https://doi.org/10.5194/amt-16-1323-2023-supplement

Atmospheric Measurement Techniques
Open Access

Supplement of

The AERosol and TRACe gas Collector (AERTRACC): an online-measurement-controlled sampler for source-resolved emission analysis

Julia Pikmann et al.

Correspondence to: Frank Drewnick (frank.drewnick@mpic.de)

S1 Calculation of PM_1 mass concentrations

The PM_1 mass concentrations were calculated from the combined particle number size distributions of FMPS (d_p = 5.6 - 560 nm) and OPC (d_p = 0.25 - 32 µm) assuming spherical particles with a density calculated based on the AMS and black carbon data using the equation of Kuwata et al. (2012) for organic density and Salcedo et al. (2006) for overall density. Since we found that the FMPS under-measures the concentrations in the uppermost size channels these were corrected using the lower OPC size channels. Details on OPC data treatment like the conversion from optical diameter to geometric diameter are provided in Drewnick et al. (2020). The uncertainty for the calculated PM_1 mass concentration is 25%. It was calculated by error propagation from the uncertainty of the density (15%) and the uncertainty of the FMPS and OPC data merging (20%).

S2 AMS and PMF data analysis

For the AMS data analysis all standard analysis procedure steps were performed with SQUIRREL 1.63I and PIKA 1.23I. A collection efficiency of 0.5 (Canagaratna et al., 2007) was applied and ionization efficiency (IE) and relative ionization efficiency (RIE) were determined in calibrations before the measurements. Elemental ratios were calculated based on the improved calibration method (Canagaratna et al., 2015).

For PMF analysis of the organic aerosol, the high-resolution data with error matrix were prepared with PIKA 1.23I. Ions with signal-to-noise ratio (SNR) < 2 were downweighted through increase of the corresponding error by a factor of 2, while ions with SNR < 0.2 were discarded from the data. The CO_2^+ ion and related ions (m/z 16, 17, 18 and 28) were downweighted by a factor of SQRT(5) as they all contain the same information. Additionally, “noisy” ions without contribution to the total measured signal were discarded. To find a robust solution the analysis was run for 1 to 7 factor solutions, with fpeak -1 to 1 (steps of 0.1) and seed 0 to 50 (steps of 1). For further analysis, the three-factor solution was chosen with fpeak=0 and seed=0. The solution was chosen based on comparison of the time series (Fig. S1a) with those of other instrument data and of the mass spectra (Fig. S1b) with literature references (Fig. S2). The residual mass is smaller than 1 %.

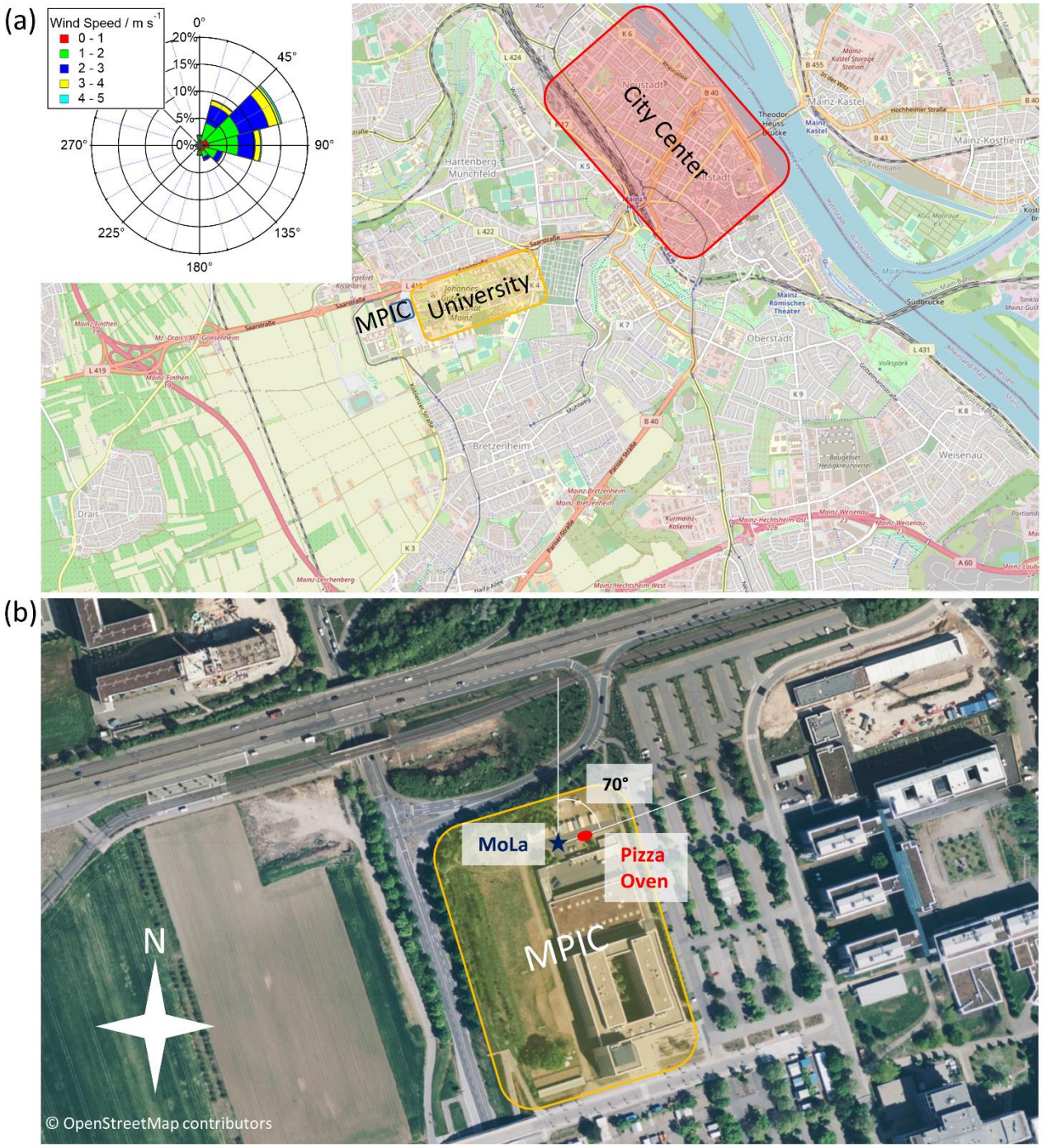

Figure S1: Site map with the location of the institute (MPIC) within the city and a wind rose plot (a) and a magnification to show the location of MoLa and the pizza oven on the premises of the institute (Source: © OpenStreetMap contributors).

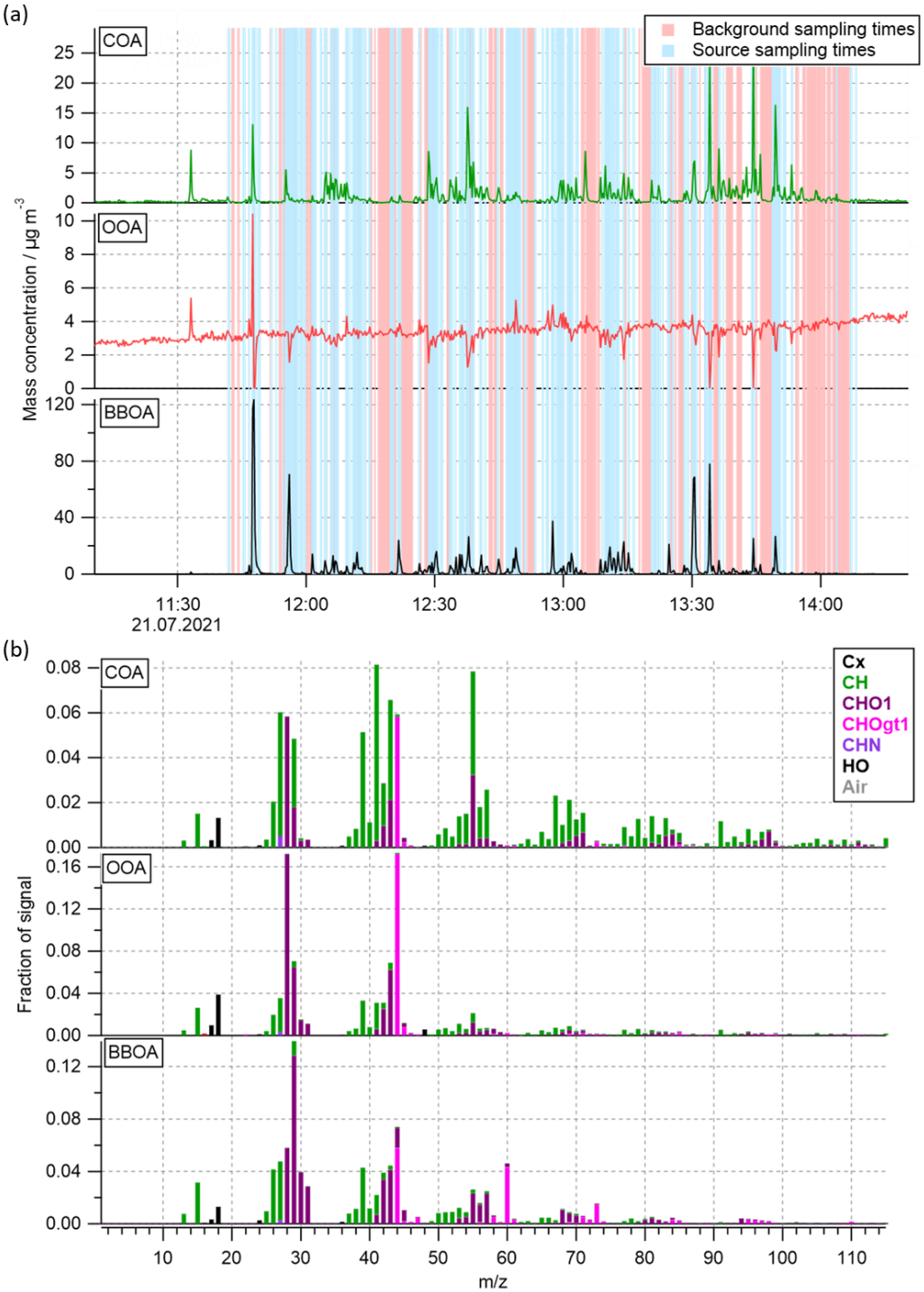

Figure S2: Time series (a) and mass spectra with the source and background aerosol sampling times highlighted in blue and red (b) of the chosen 3-factor solution of the PMF analysis representing the three different aerosol types, observed during the field-validation measurement.

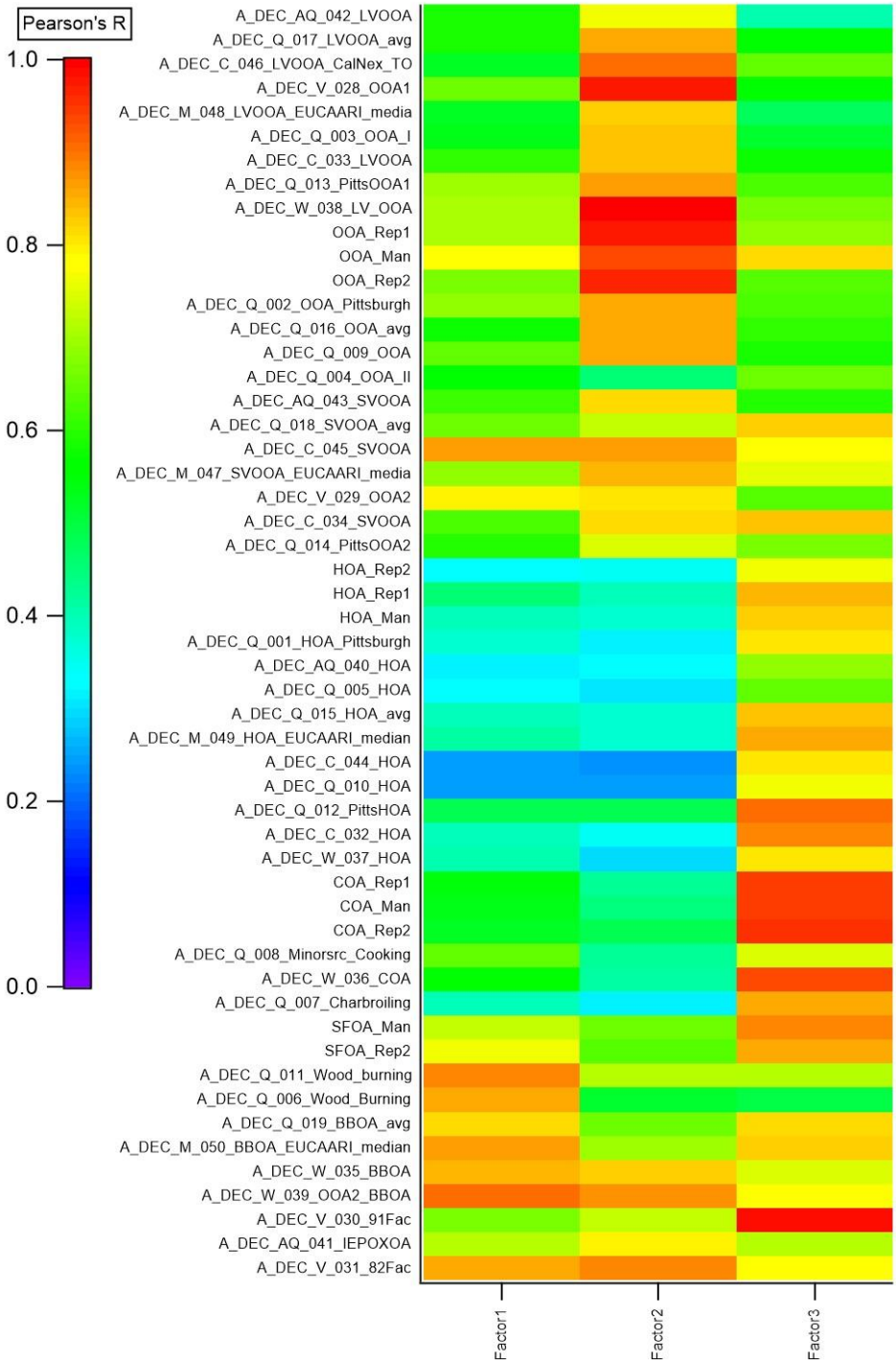

Figure S3: Comparison of the three PMF factor mass spectra with reference spectra. Shown are Pearson R values from correlation of the PMF factor mass spectra with different reference mass spectra from the AMS Spectral Database (Ulbrich et al., 2022) as color-coded boxes.

S3 CIMS data analysis

For the CIMS data analysis, the software Tofware 3.2.3 (Aerodyne Inc., USA) and custom data procedures were used. All standard analysis procedure steps were performed including m/z calibration (with $I(H_2O)^-$, $I(CH_2O_2)^-$, $I(HNO_3)^-$, I_2^- and I_3^-, deviation < 3 ppm), background correction using the field blanks and normalization to the iodide signal.

S4 Error calculation for Fig. 4

To determine the reproducibility, several samples were prepared with equal sample amounts by simultaneously sampling the same aerosol onto multiple filters and TDTs. For the overall reproducibility, the standard deviation over all samples for all individual compounds, which were identified in this study (Section 4), was calculated and then these standard deviations were averaged over all compounds.

As error for the signal intensity of individual compounds the uncertainty, derived from the reproducibility determination, and the error from a Gaussian error propagation of the standard deviation of the blanks and the samples were compared and the larger one was chosen. The signal intensity from compounds found on blank filters was negligible in contrast to source and background samples. The error for the ratios was calculated using Gaussian error propagation from the errors of signal intensity of source and background samples. Error bars of the overall source ratios represent the standard error of the ratios of all ions assigned to the respective sources.

S5 Additional figures and tables

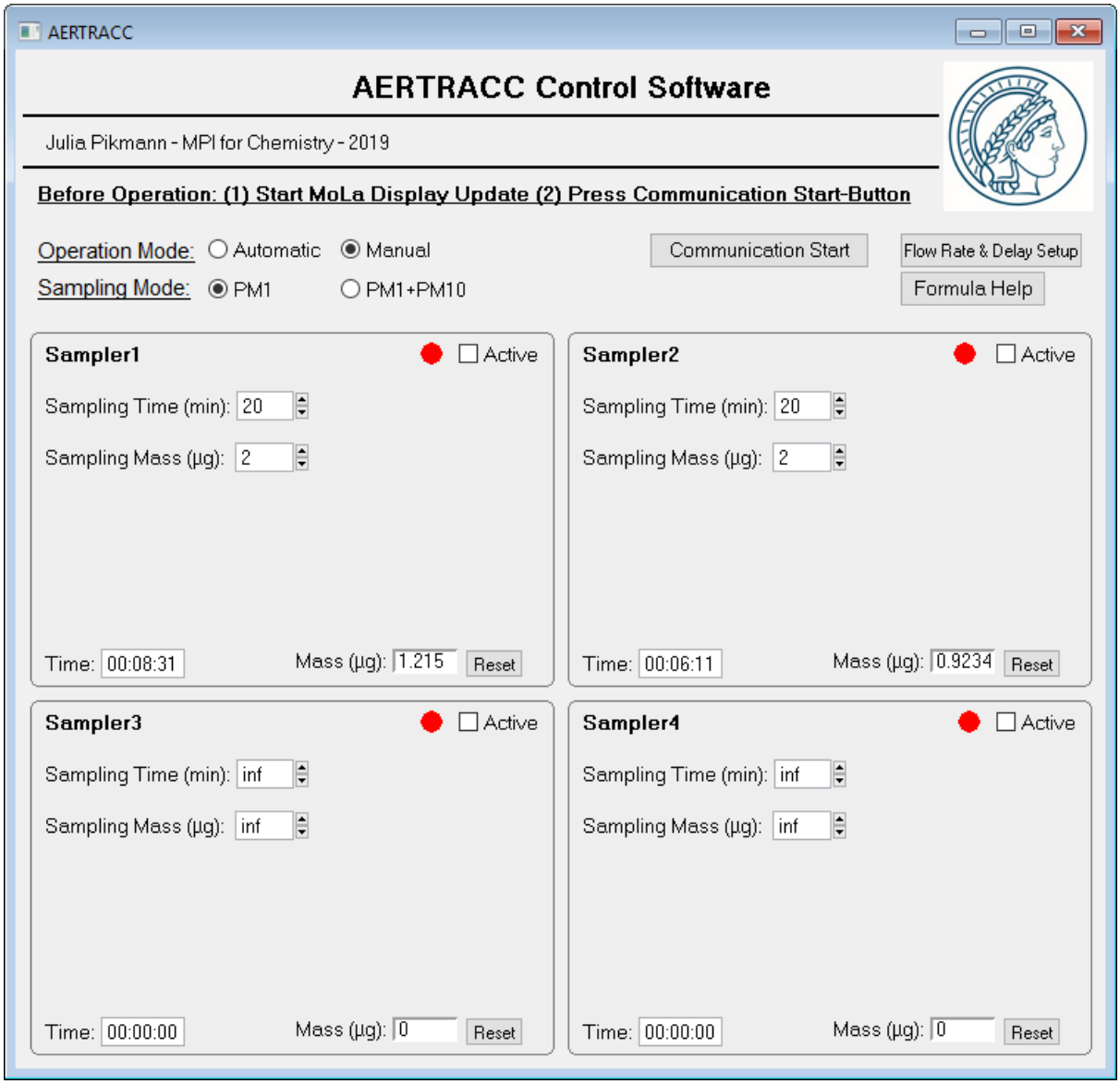

Figure S4: User interface of the AERTRACC software in manual sampling mode. For each sampling path, a sampling time and mass limit can be set. To sample, the "Active" checkbox needs to be checked; then the red indicator for "non-sampling" turns green for "sampling". For each sampling path, two displays show the current accumulated collection time and accumulated aerosol mass. The panel for automatic sampling mode is shown in the main text.

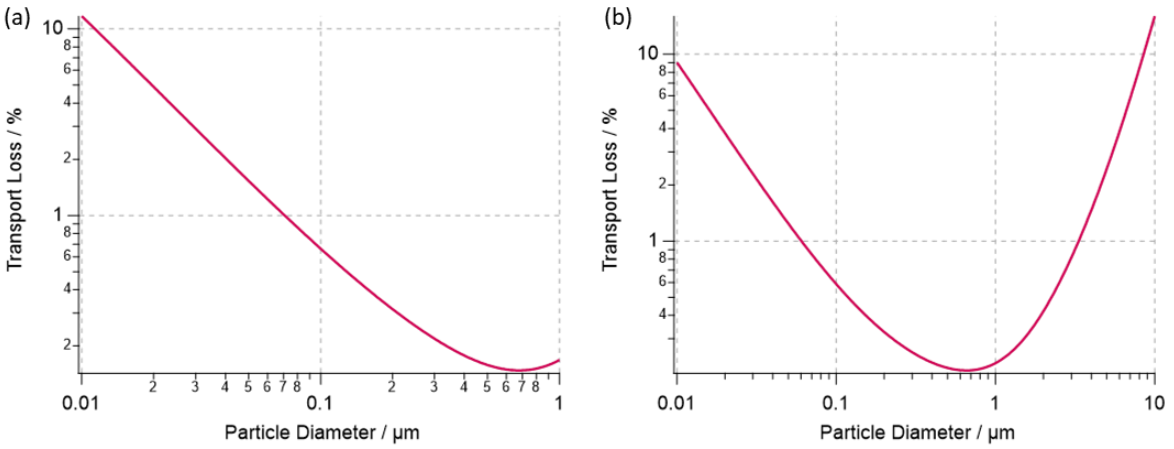

Figure S5: Size-dependent transport losses for the (a) PM_1-only and (b) PM_1/PM_{10} sampling mode. For the calculations, it was assumed that the particles are spherical with a density of 1 g cm^{-3}. The considered particle loss mechanisms are diffusion, sedimentation, and inertial deposition.

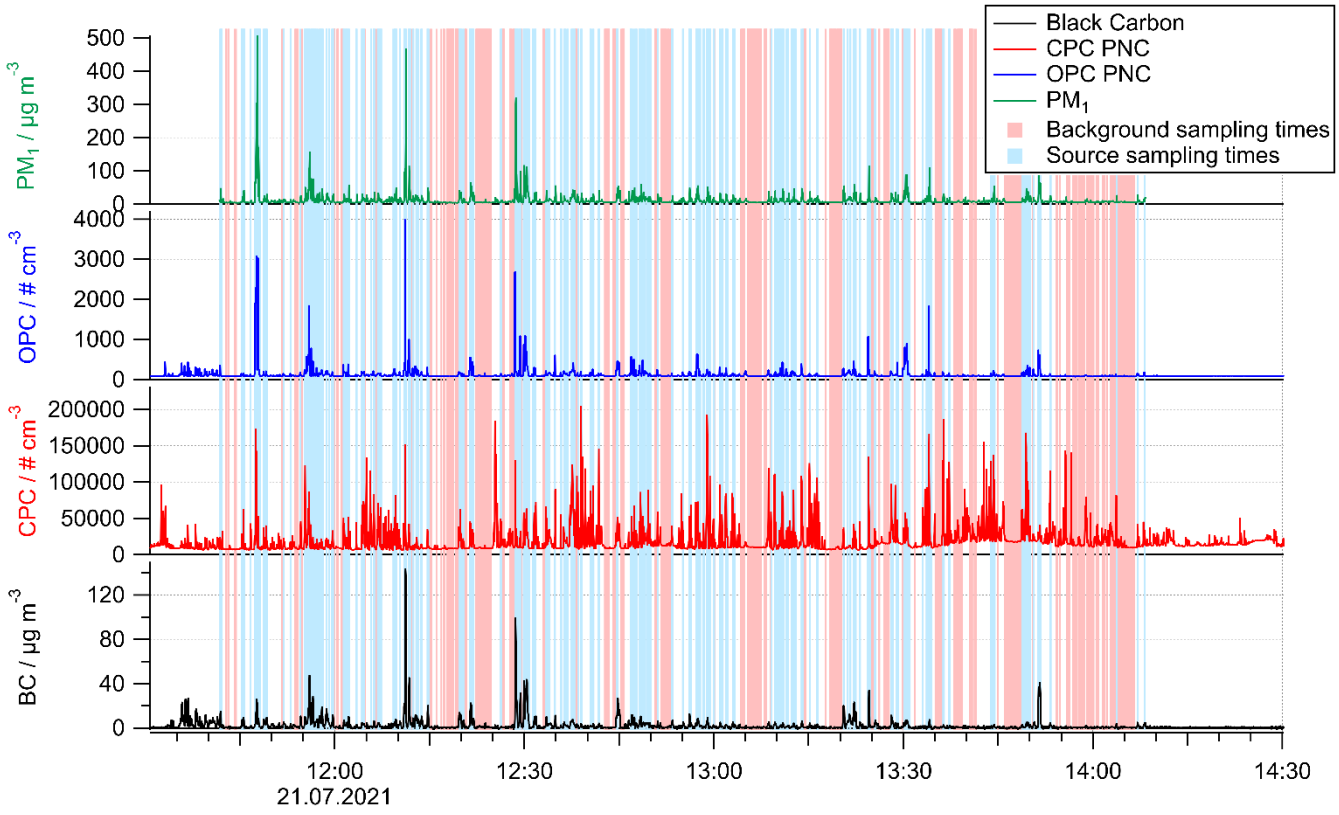

Figure S6: Time series for the relevant parameters black carbon and PM_1 mass concentration as well as CPC and OPC particle number concentration. The source and background aerosol sampling times are highlighted in blue and red.

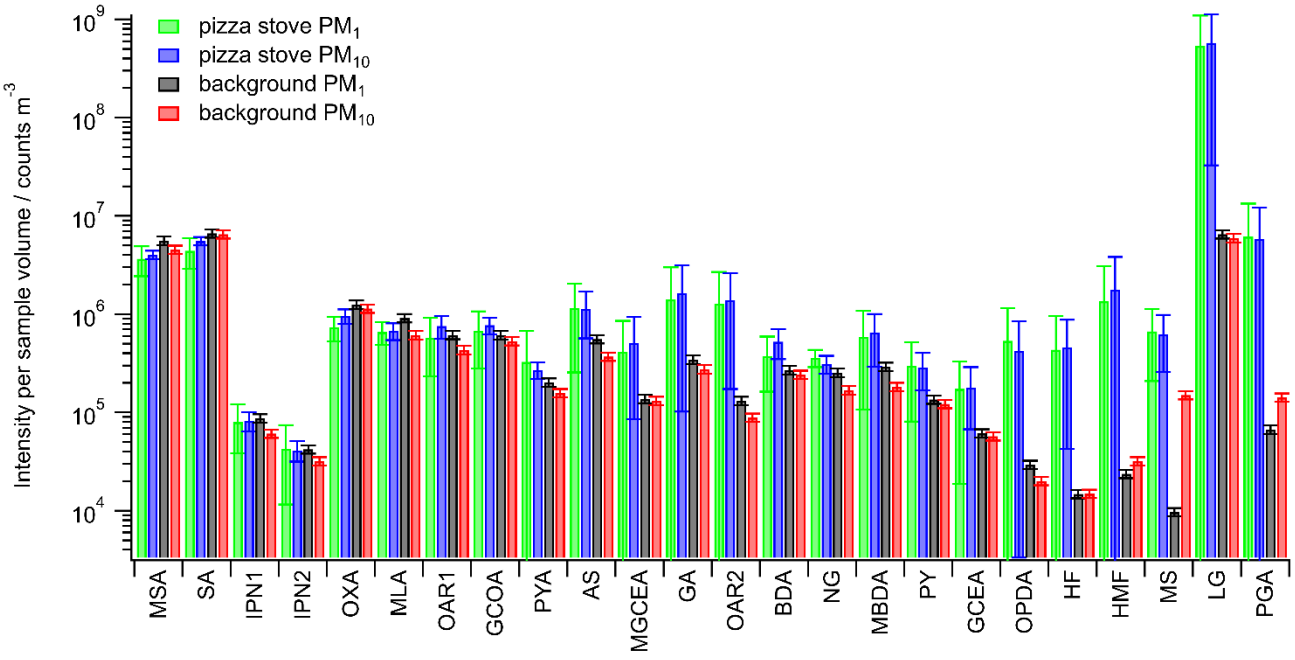

Figure S7: Ion signal intensities normalized to the respective sampled volume for the PM_1 and PM_{10} filters from pizza oven and background sampling. Error Bars show the larger uncertainty, either the reproducibility or the uncertainty estimated by error propagation from the standard deviation of the blank and the ambient measurements.

Table S1: List of identified compounds from filter analysis with acronyms used in the main text, molecular formula of the respective detected ion, and assigned sources based on the quoted references.

m/z	Detected ion	Assigned compound	Acronym	Assigned sources	Reference
202.92107	$IC_2H_4O_3^-$	glycolic acid	GCOA	biomass burning, cooking emissions	Coggon et al., 2019; Lim et al., 2005; Reyes-Villegas et al., 2018
212.90541	$IC_3H_2O_3^-$	oxopropanedial, oxoacrylic acid	OPDA	biomass burning	Alves et al., 2010; Zhao et al., 2014
214.92107	$IC_3H_4O_3^-$	pyruvic acid	PYA	biomass burning, cooking emissions	Abdullahi et al., 2013; Coggon et al., 2019; Lim et al., 2005; Permar et al., 2021; Reyes-Villegas et al., 2018; Wang et al., 2006
216.90033	$IC_2H_2O_4^-$	oxalic acid	OXA	biomass burning, vehicle emissions	Huang and Yu, 2007; Lim et al., 2005; Wang et al., 2006; Zhou et al., 2015
222.89314	$ICH_4O_3S^-$	methanesulfonic acid	MSA	aged aerosol	Perraud et al., 2015
224.87241	$IH_2O_4S^-$	sulfuric acid	SA	oxidation of SO_2	Perraud et al., 2015
232.93163	$IC_3H_6O_4^-$	glyceric acid	GCEA	cooking emissions	Reyes-Villegas et al., 2018
238.92107	$IC_5H_4O_3^-$	hydroxy furfural, furoic acid	HF/FA	biomass burning	Permar et al., 2021
242.91599	$IC_4H_4O_4^-$	butenedioic acid	BDA	biomass burning	Di Hu and Yu, 2013; Röhrl and Lammel, 2002; Ye et al., 2021
246.947	$IC_4H_8O_4^-$	methylglyceric acid	MGCEA	aged aerosol, cooking emission	Reyes-Villegas et al., 2018; Szmigielski et al., 2007
252.93672	$IC_6H_6O_3^-$	hydroxymethyl furfural	HMF	biomass burning	Permar et al., 2021; Yee et al., 2013
255.94762	$IC_5H_7NO_3^-$	pyroglutamic acid	PGA	cooking emissions	Reyes-Villegas et al., 2018
256.93164	$IC_5H_6O_4^-$	methylbutendioic acid	MBDA	biomass burning	Coggon et al., 2019; Ye et al., 2021
258.94727	$IC_5H_8O_4^-$	glutaric acid	GA	biomass burning, cooking emissions	Coggon et al., 2019; Reyes-Villegas et al., 2018; Wang et al., 2006

260.92654	$IC_4H_6O_5^-$	malic acid	MLA	biomass burning, vehicle emissions	Röhrl and Lammel, 2002; Wang et al., 2006
268.93164	$IC_6H_6O_4^-$	oxidized aromats	OAR2	aged aerosol, biomass burning	Yee et al., 2013
276.95786	$IC_5H_{10}O_5^-$	pyranose	PY	biomass burning, cooking emissions	Chen et al., 2020; Reyes-Villegas et al., 2018; Simoneit et al., 2000
288.95786	$IC_6H_{10}O_5^-$	levoglucosan, galactosan, mannosan	LG	biomass burning, cooking emissions	Abdullahi et al., 2013; Gaston et al., 2016; Křůmal et al., 2019; Reyes-Villegas et al., 2018
295.94254	$IC_7H_7NO_4^-$	nitroguaiacol	NG	biomass burning	Coggon et al., 2019; Lauraguais et al., 2014
300.95786	$IC_7H_{10}O_5^-$	oxidized aromats, 3-acetylpentane-dioic acid	OAR1	aged aerosol, biomass burning	Chen et al., 2020; Yee et al., 2013
302.9371	$IC_6H_8O_6^-$	ascorbic acid, hydroxyfurans	AS	biomass burning, vehicle emissions	Priestley et al., 2021
303.93234	$IC_5H_7NO_6^-$	oxidized isoprene nitrate	IPN1	aged aerosol	Zhao et al., 2021
305.948	$IC_5H_9NO_6^-$	oxidized isoprene nitrate	IPN2	aged aerosol	Zhao et al., 2021
306.96841	$IC_6H_{12}O_6^-$	monosaccharide	MS	biomass burning, cooking emissions	Gaston et al., 2016; Ye et al., 2021

Table S2: List of identified compounds from TDT analysis with acronyms used in the main text, molecular formula of the respective detected ion, and assigned sources based on the quoted references.

m/z	Detected ion	Assigned compound	Acronym	Assigned sources	Reference
171.926	ICH_3NO^-	formamide	FM	biomass burning, aged aerosol	Permar et al., 2021; Priestley et al., 2018; Schwantes et al., 2019; Ye et al., 2021
186.926	$IC_2H_4O_2^-$	acetic acid	AA	biomass burning, aged aerosol, traffic	Kong et al., 2021; Liggio et al., 2017; Lim et al., 2005; Permar et al., 2021; Ye et al., 2021
188.942	$IC_2H_6O_2^-$	ethylene glycol	EG	aged aerosol, biomass burning	Duncan et al., 2019; Kong et al., 2021; Reyes-Villegas et al., 2018; Schulten and Schurath, 1975
199.921	$IC_2H_3NO_2^-$	N-formylformamide, nitroethen	FFM	biomass burning	Permar et al., 2021; Priestley et al., 2018
200.942	$IC_3H_6O_2^-$	propanoic acid	PA	biomass burning, cooking, aged aerosol	Bi et al., 2022; Jia and Xu, 2018; Priestley et al., 2018; Reyes-Villegas et al., 2018
202.957	$IC_3H_8O_2^-$	propandiol, hydroxyacetone	PDO	aged aerosol	Mehra et al., 2020; Schulten and Schurath, 1975
212.905	$IC_3H_2O_3^-$	oxopropanedial, oxoacrylic acid	OPDA	biomass burning	Alves et al., 2010; Craven et al., 2012; Du et al., 2021; Zhao et al., 2014
214.921	$IC_3H_4O_3^-$	pyruvic acid	PYA	biomass burning, cooking emission, traffic	Abdullahi et al., 2013; Coggon et al., 2019; Lim et al., 2005; Permar et al., 2021; Reyes-Villegas et al., 2018; Wang et al., 2006
214.957	$IC_4H_8O_2^-$	butyric acid, methyl propanoate	BA	biomass burning, traffic	Duncan et al., 2019; Liggio et al., 2017; Permar et al., 2021; Priestley et al., 2018
224.942	$IC_5H_6O_2^-$	furfuryl alcohol, 2-furanmethanol	FFA	biomass burning, aged aerosol	Kong et al., 2021; Nguyen et al., 2011; Permar et al., 2021; Priestley et al., 2018
230.989	$IC_5H_{12}O_2^-$	alkyldiole	OAL3	traffic	Grayson et al., 2016; Schröder et al., 2016; Sutapa et al., 2021

234.963	$IC_7H_8O^-$	cresol	CRES	biomass burning, cooking, aged aerosol	Klein et al., 2016; Mutzel et al., 2021; Permar et al., 2021
240.973	$IC_6H_{10}O_2^-$	hexanoic acid, cyclopentanoic acid	HA	biomass burning, traffic	Abdullahi et al., 2013; Liggio et al., 2017; Reyes-Villegas et al., 2018
252.973	$IC_7H_{10}O_2^-$	Cyclohexene- carboxylic acid	CHCA	traffic, aged aerosol	Hammes et al., 2018; Liggio et al., 2017; Smith et al., 2020
256.968	$IC_6H_{10}O_3^-$	oxohexanoic acid, ethyl acetoacetate, methyloxopenta-noic acid	OHA	biomass burning, cooking, aged aerosol	Boris et al., 2016; Duncan et al., 2019; Kong et al., 2021
269.004	$IC_8H_{14}O_2^-$	oxidized alkane	OAL4	aged aerosol	Craven et al., 2012; Shao et al., 2022
270.984	$IC_7H_{12}O_3^-$	oxidized alkane	OAL2	aged aerosol	Hammes et al., 2018; Mackenzie-Rae et al., 2018
271.020	$IC_8H_{16}O_2^-$	octanoic acid	OA	traffic, cooking	Abdullahi et al., 2013; Schauer et al., 1999, 2002a, 2002b
275.974	$IC_5H_{11}NO_4^-$	oxidized alkane	OAL1	aged aerosol	Link, 2019
283.020	$IC_9H_{16}O_2^-$	nonenoic acid	NA	aged aerosol	Hamilton et al., 2011; Qi et al., 2020
292.953	$IC_5H_{10}O_6^-$	sugar acid	SUGA	cooking	Kurtén et al., 2018; Reyes-Villegas et al., 2018
296.999	$IC_9H_{14}O_3^-$	pinalic-3-acid, limonalic acid	PINA	cooking, aged aerosol	Hammes et al., 2018; Reyes-Villegas et al., 2018
297.036	$IC_{10}H_{18}O_2^-$	decenoic acid, pinanediol, linalool oxide	DCA	aged aerosol	Bi et al., 2022; Kirkby and Collaboration, 2013; Rondo et al., 2014
299.051	$IC_{10}H_{20}O_2^-$	decanoic acid	DA	traffic	Schauer et al., 1999, 2002a, 2002b; Sutapa et al., 2021
311.015	$IC_{10}H_{16}O_3^-$	oxocarboxylic acid	OCA	aged aerosol, traffic, cooking	Hammes et al., 2018; Kong et al., 2021; Liggio et al., 2017; Reyes-Villegas et al., 2018; Ye et al., 2021
327.083	$IC_{12}H_{24}O_2^-$	dodecanoic acid, methylundeca-noic acid	DDA	traffic, cooking	Schauer et al., 1999, 2002a; Sutapa et al., 2021
363.083	$IC_{15}H_{24}O_2^-$	β-caryophyllene-aldehyde	CPA	aged aerosol	Gao et al., 2022; Li et al., 2011

Table S3: Average concentrations of potentially source-related aerosol components and total source-related sampling time for the three-divided wind sectors in comparison to the undivided wind sector and the combined wind sector + OPC sampling condition.

	45-60°	60-75°	75-90°	Wind (45-90°)	Wind+OPC
Black Carbon (ng m^{-3})	2.7	3.3	3.1	3.1	22.0
CPC (# cm^{-3})	1.5	1.9	1.8	1.7	2.8
PAH (ng m^{-3})	2.1	2.6	2.9	2.5	13.4
PM1 (µg m^{-3})	2.3	2.9	2.4	2.5	5.2
Organics (µg m^{-3})	1.7	2.0	2.0	1.9	3.5
OPC (# cm^{-3})	1.6	1.8	1.8	1.7	22.0
BBOA (µg m^{-3})	3.6	5.6	5.6	4.9	1.3
OOA (µg m^{-3})	3.5	3.5	3.5	3.5	3.7
COA (µg m^{-3})	1.2	1.7	1.9	1.6	1.0
Sampling Time (s)	1198	1273	1087	3779	979

Table S4: Average concentrations of potentially source-related aerosol components and total source-related sampling time for the five-divided wind sectors in comparison to the undivided wind sector and the combined wind sector + OPC sampling condition.

	45-54°	54-63°	63-72°	72-81°	81-90°	Wind (45-90°)	Wind+OPC
Black Carbon (ng m^{-3})	2.7	2.8	3.5	3.1	3.1	3.1	22.0
CPC (# cm^{-3})	1.4	1.7	1.9	1.9	1.7	1.7	2.8
PAH (ng m^{-3})	2.1	2.4	2.6	2.9	2.6	2.5	13.4
PM1 (µg m^{-3})	2.4	2.3	3.0	2.6	2.2	1.7	5.2
Organics (µg m^{-3})	1.7	1.8	2.0	2.2	1.7	1.9	3.5
OPC (# cm^{-3})	1.6	1.6	1.9	2.0	1.4	1.7	22.0
BBOA (µg m^{-3})	3.3	4.1	6.0	6.5	4.5	4.9	1.3
OOA (µg m^{-3})	3.5	3.5	3.5	3.5	3.6	3.5	3.7
COA (µg m^{-3})	1.2	1.5	1.6	2.0	1.8	1.6	1.0
Sampling Time (s)	700	757	759	733	609	3779	979

Table S5: Average concentrations of potentially source-related aerosol components and total source-related sampling time for the seven-divided wind sectors in comparison to the undivided wind sector and the combined wind sector + OPC sampling condition.

	45-51°	51-58°	58-64°	64-71°	71-77°	77-84°	84-90°	Wind (45-90°)	Wind+OPC
Black Carbon (ng m^{-3})	2.8	2.4	3.1	3.7	3.0	2.8	3.5	3.1	22.0
CPC (# cm^{-3})	1.4	1.6	1.8	1.9	1.9	1.8	1.7	1.7	2.8
PAH (ng m^{-3})	2.1	2.1	2.4	2.9	2.7	2.6	3.0	2.5	13.4

PM1 (μg m^{-3})	2.3	2.3	2.9	2.8	2.8	2.3	2.2	1.7	5.2
Organics (μg m^{-3})	1.7	1.5	2.0	2.0	2.2	1.8	1.8	1.9	3.5
OPC (# cm^{-3})	1.6	1.5	1.7	1.8	2.0	1.7	1.4	1.7	22.0
BBOA (μg m^{-3})	3.2	3.1	5.8	5.3	6.9	5.1	4.7	4.9	1.3
OOA (μg m^{-3})	3.5	3.5	3.5	3.6	3.5	3.6	3.5	3.5	3.7
COA (μg m^{-3})	1.1	1.2	1.9	1.5	2.0	1.8	1.9	1.6	1.0
Sampling Time (s)	527	497	607	511	555	466	395	3779	979

References

Aljawhary, D., Lee, A. K. Y., and Abbatt, J. P. D.: High-resolution chemical ionization mass spectrometry (ToF-CIMS): application to study SOA composition and processing, Atmos. Meas. Tech., 6, 3211–3224, https://doi.org/10.5194/amt-6-3211-2013, 2013.

Bai, Z., Ji, Y., Pi, Y., Yang, K., Wang, L., Zhang, Y., Zhai, Y., Yan, Z., and Han, X.: Hygroscopic analysis of individual Beijing haze aerosol particles by environmental scanning electron microscopy, Atmospheric Environment, 172, 149–156, https://doi.org/10.1016/j.atmosenv.2017.10.031, 2018.

Bhowmik, H. S., Shukla, A., Lalchandani, V., Dave, J., Rastogi, N., Kumar, M., Singh, V., and Tripathi, S. N.: Inter-comparison of online and offline methods for measuring ambient heavy and trace elements and water-soluble inorganic ions (NO_3^-, SO_4^{2-}, NH_4^+, and Cl^-) in $PM_{2.5}$ over a heavily polluted megacity, Delhi, Atmos. Meas. Tech., 15, 2667–2684, https://doi.org/10.5194/amt-15-2667-2022, 2022.

Canagaratna, M. R., Jayne, J. T., Jimenez, J. L., Allan, J. D., Alfarra, M. R., Zhang, Q., Onasch, T. B., Drewnick, F., Coe, H., Middlebrook, A., Delia, A., Williams, L. R., Trimborn, A. M., Northway, M. J., DeCarlo, P. F., Kolb, C. E., Davidovits, P., and Worsnop, D. R.: Chemical and microphysical characterization of ambient aerosols with the aerodyne aerosol mass spectrometer, Mass spectrometry reviews, 26, 185–222, https://doi.org/10.1002/mas.20115, 2007.

Celik, S., Drewnick, F., Fachinger, F., Brooks, J., Darbyshire, E., Coe, H., Paris, J.-D., Eger, P. G., Schuladen, J., Tadic, I., Friedrich, N., Dienhart, D., Hottmann, B., Fischer, H., Crowley, J. N., Harder, H., and Borrmann, S.: Influence of vessel characteristics and atmospheric processes on the gas and particle phase of ship emission plumes: in situ measurements in the Mediterranean Sea and around the Arabian Peninsula, Atmos. Chem. Phys., 20, 4713–4734, https://doi.org/10.5194/acp-20-4713-2020, 2020.

DeCarlo, P. F., Kimmel, J. R., Trimborn, A., Northway, M. J., Jayne, J. T., Aiken, A. C., Gonin, M., Fuhrer, K., Horvath, T., Docherty, K. S., Worsnop, D. R., and Jimenez, J. L.: Field-deployable, high-resolution, time-of-flight aerosol mass spectrometer, Analytical chemistry, 78, 8281–8289, https://doi.org/10.1021/ac061249n, 2006.

Dettmer, K. and Engewald, W.: Ambient air analysis of volatile organic compounds using adsorptive enrichment, Chromatographia, 57, S339-S347, https://doi.org/10.1007/BF02492126, 2003.

Dettmer, K. and Engewald, W.: Adsorbent materials commonly used in air analysis for adsorptive enrichment and thermal desorption of volatile organic compounds, Anal. Bioanal. Chem., 373, 490–500, https://doi.org/10.1007/s00216-002-1352-5, 2002.

Drewnick, F., Böttger, T., Weiden-Reinmüller, S.-L. v. d., Zorn, S. R., Klimach, T., Schneider, J., and Borrmann, S.: Design of a mobile aerosol research laboratory and data processing tools for effective stationary and mobile field measurements, Atmos. Meas. Tech., 5, 1443–1457, https://doi.org/10.5194/amt-5-1443-2012, 2012.

Drewnick, F., Pikmann, J., Fachinger, F., Moormann, L., Sprang, F., and Borrmann, S.: Aerosol filtration efficiency of household materials for homemade face masks: Influence of material properties, particle size,

particle electrical charge, face velocity, and leaks, Aerosol Science and Technology, 55, 63–79, https://doi.org/10.1080/02786826.2020.1817846, 2020.

Ebert, M., Weigel, R., Kandler, K., Günther, G., Molleker, S., Grooß, J.-U., Vogel, B., Weinbruch, S., and Borrmann, S.: Chemical analysis of refractory stratospheric aerosol particles collected within the arctic vortex and inside polar stratospheric clouds, Atmos. Chem. Phys., 16, 8405–8421, https://doi.org/10.5194/acp-16-8405-2016, 2016.

Faber, P., Drewnick, F., Bierl, R., and Borrmann, S.: Complementary online aerosol mass spectrometry and offline FT-IR spectroscopy measurements: Prospects and challenges for the analysis of anthropogenic aerosol particle emissions, Atmospheric Environment, 166, 92–98, https://doi.org/10.1016/j.atmosenv.2017.07.014, 2017.

Fachinger, F., Drewnick, F., and Borrmann, S.: How villages contribute to their local air quality – The influence of traffic- and biomass combustion-related emissions assessed by mobile mappings of PM and its components, Atmospheric Environment, 263, 118648, https://doi.org/10.1016/j.atmosenv.2021.118648, 2021.

Fachinger, F., Drewnick, F., Gieré, R., and Borrmann, S.: How the user can influence particulate emissions from residential wood and pellet stoves: Emission factors for different fuels and burning conditions, Atmospheric Environment, 158, 216–226, https://doi.org/10.1016/j.atmosenv.2017.03.027, 2017.

Forbes, P.: Atmospheric Chemistry Analysis: A Review, Analytical chemistry, 92, 455–472, https://doi.org/10.1021/acs.analchem.9b04623, 2020.

Fuzzi, S., Baltensperger, U., Carslaw, K., Decesari, S., van der Denier Gon, H., Facchini, M. C., Fowler, D., Koren, I., Langford, B., Lohmann, U., Nemitz, E., Pandis, S., Riipinen, I., Rudich, Y., Schaap, M., Slowik, J. G., Spracklen, D. V., Vignati, E., Wild, M., Williams, M., and Gilardoni, S.: Particulate matter, air quality and climate: lessons learned and future needs, Atmos. Chem. Phys., 15, 8217–8299, https://doi.org/10.5194/acp-15-8217-2015, 2015.

Gilardoni, S.: Advances in organic aerosol characterization: From complex to simple, Aerosol Air Qual. Res., 17, 1447–1451, https://doi.org/10.4209/aaqr.2017.01.0007, 2017.

Gordon, H., Kirkby, J., Baltensperger, U., Bianchi, F., Breitenlechner, M., Curtius, J., Dias, A., Dommen, J., Donahue, N. M., Dunne, E. M., Duplissy, J., Ehrhart, S., Flagan, R. C., Frege, C., Fuchs, C., Hansel, A., Hoyle, C. R., Kulmala, M., Kürten, A., Lehtipalo, K., Makhmutov, V., Molteni, U., Rissanen, M. P., Stozkhov, Y., Tröstl, J., Tsagkogeorgas, G., Wagner, R., Williamson, C., Wimmer, D., Winkler, P. M., Yan, C., and Carslaw, K. S.: Causes and importance of new particle formation in the present-day and preindustrial atmospheres, J. Geophys. Res., 122, 8739–8760, https://doi.org/10.1002/2017JD026844, 2017.

Hallquist, M., Wenger, J. C., Baltensperger, U., Rudich, Y., Simpson, D., Claeys, M., Dommen, J., Donahue, N. M., George, C., Goldstein, A. H., Hamilton, J. F., Herrmann, H., Hoffmann, T., Iinuma, Y., Jang, M., Jenkin, M. E., Jimenez, J. L., Kiendler-Scharr, A., Maenhaut, W., McFiggans, G., Mentel, T. F., Monod, A., Prévôt, A. S. H., Seinfeld, J. H., Surratt, J. D., Szmigielski, R., and Wildt, J.: The formation, properties and impact of secondary organic aerosol: current and emerging issues, Atmos. Chem. Phys., 9, 5155–5236, https://doi.org/10.5194/acp-9-5155-2009, 2009.

Harper, M.: Sorbent trapping of volatile organic compounds from air, J. Chromatogr. A, 885, 129–151, https://doi.org/10.1016/S0021-9673(00)00363-0, 2000.

Heard, D. E.: Analytical techniques for atmospheric measurement, Blackwell Pub, Ames, Iowa, 510 pp., 2006.

Johnston, M. V. and Kerecman, D. E.: Molecular Characterization of Atmospheric Organic Aerosol by Mass Spectrometry, Annual review of analytical chemistry (Palo Alto, Calif.), 12, 247–274, https://doi.org/10.1146/annurev-anchem-061516-045135, 2019.

Kuwata, M., Zorn, S. R., and Martin, S. T.: Using elemental ratios to predict the density of organic material composed of carbon, hydrogen, and oxygen, Environmental science & technology, 46, 787–794, https://doi.org/10.1021/es202525q, 2012.

Laskin, J., Laskin, A., and Nizkorodov, S. A.: Mass Spectrometry Analysis in Atmospheric Chemistry, Analytical chemistry, 90, 166–189, https://doi.org/10.1021/acs.analchem.7b04249, 2018.

Lee, B. H., Lopez-Hilfiker, F. D., Mohr, C., Kurtén, T., Worsnop, D. R., and Thornton, J. A.: An iodide-adduct high-resolution time-of-flight chemical-ionization mass spectrometer: application to atmospheric inorganic and organic compounds, Environmental science & technology, 48, 6309–6317, https://doi.org/10.1021/es500362a, 2014.

Lopez-Hilfiker, F. D., Mohr, C., Ehn, M., Rubach, F., Kleist, E., Wildt, J., Mentel, T. F., Lutz, A., Hallquist, M., Worsnop, D., and Thornton, J. A.: A novel method for online analysis of gas and particle composition: description and evaluation of a Filter Inlet for Gases and AEROsols (FIGAERO), Atmos. Meas. Tech., 7, 983–1001, https://doi.org/10.5194/amt-7-983-2014, 2014.

Mercier, F., Glorennec, P., Blanchard, O., and Le Bot, B.: Analysis of semi-volatile organic compounds in indoor suspended particulate matter by thermal desorption coupled with gas chromatography/mass spectrometry, Journal of chromatography. A, 1254, 107–114, https://doi.org/10.1016/j.chroma.2012.07.025, 2012.

Ng, N. L., Canagaratna, M. R., Zhang, Q., Jimenez, J. L., Tian, J., Ulbrich, I. M., Kroll, J. H., Docherty, K. S., Chhabra, P. S., Bahreini, R., Murphy, S. M., Seinfeld, J. H., Hildebrandt, L., Donahue, N. M., DeCarlo, P. F., Lanz, V. A., Prévôt, A. S. H., Dinar, E., Rudich, Y., and Worsnop, D. R.: Organic aerosol components observed in Northern Hemispheric datasets from Aerosol Mass Spectrometry, Atmos. Chem. Phys., 10, 4625–4641, https://doi.org/10.5194/acp-10-4625-2010, 2010.

Paatero, P. and Tapper, U.: Positive matrix factorization: A non-negative factor model with optimal utilization of error estimates of data values, Environmetrics, 5, 111–126, https://doi.org/10.1002/env.3170050203, 1994.

Parshintsev, J. and Hyötyläinen, T.: Methods for characterization of organic compounds in atmospheric aerosol particles, Anal. Bioanal. Chem., 407, 5877–5897, https://doi.org/10.1007/s00216-014-8394-3, 2015.

Schneider, J., Weimer, S., Drewnick, F., Borrmann, S., Helas, G., Gwaze, P., Schmid, O., Andreae, M. O., and Kirchner, U.: Mass spectrometric analysis and aerodynamic properties of various types of combustion-related aerosol particles, International Journal of Mass Spectrometry, 258, 37–49, https://doi.org/10.1016/j.ijms.2006.07.008, 2006.

Shrivastava, M., Cappa, C. D., Fan, J., Goldstein, A. H., Guenther, A. B., Jimenez, J. L., Kuang, C., Laskin, A., Martin, S. T., Ng, N. L., Petaja, T., Pierce, J. R., Rasch, P. J., Roldin, P., Seinfeld, J. H., Shilling, J., Smith, J. N., Thornton, J. A., Volkamer, R., Wang, J., Worsnop, D. R., Zaveri, R. A., Zelenyuk, A., and Zhang, Q.: Recent advances in understanding secondary organic aerosol: Implications for global climate forcing, Rev. Geophys., 55, 509–559, https://doi.org/10.1002/2016RG000540, 2017.

Stavroulas, I., Bougiatioti, A., Grivas, G., Paraskevopoulou, D., Tsagkaraki, M., Zarmpas, P., Liakakou, E., Gerasopoulos, E., and Mihalopoulos, N.: Sources and processes that control the submicron organic aerosol composition in an urban Mediterranean environment (Athens): a high temporal-resolution chemical composition measurement study, Atmos. Chem. Phys., 19, 901–919, https://doi.org/10.5194/acp-19-901-2019, 2019.

Struckmeier, C., Drewnick, F., Fachinger, F., Gobbi, G. P., and Borrmann, S.: Atmospheric aerosols in Rome, Italy: sources, dynamics and spatial variations during two seasons, Atmos. Chem. Phys., 16, 15277–15299, https://doi.org/10.5194/acp-16-15277-2016, 2016.

Sun, Y.-L., Zhang, Q., Schwab, J. J., Demerjian, K. L., Chen, W.-N., Bae, M.-S., Hung, H.-M., Hogrefe, O., Frank, B., Rattigan, O. V., and Lin, Y.-C.: Characterization of the sources and processes of organic and inorganic aerosols in New York city with a high-resolution time-of-flight aerosol mass apectrometer, Atmos. Chem. Phys., 11, 1581–1602, https://doi.org/10.5194/acp-11-1581-2011, 2011.

Ulbrich, I. M., Handschy, A., Lechner, M., and Jimenez, J.L.: High-Resolution AMS Spectral Database, 2022.

Ulbrich, I. M., Canagaratna, M. R., Zhang, Q., Worsnop, D. R., and Jimenez, J. L.: Interpretation of organic components from Positive Matrix Factorization of aerosol mass spectrometric data, Atmos. Chem. Phys., 9, 2891–2918, https://doi.org/10.5194/acp-9-2891-2009, 2009.

von der Weiden, S.-L., Drewnick, F., and Borrmann, S.: Particle Loss Calculator – a new software tool for the assessment of the performance of aerosol inlet systems, Atmos. Meas. Tech., 2, 479–494, https://doi.org/10.5194/amt-2-479-2009, 2009.

Williams, B. J., Goldstein, A. H., Kreisberg, N. M., and Hering, S. V.: An In-Situ Instrument for Speciated Organic Composition of Atmospheric Aerosols: Thermal Desorption Aerosol GC/MS-FID (TAG), Aerosol Sci. Technol., 40, 627–638, https://doi.org/10.1080/02786820600754631, 2006.

Woolfenden, E.: Sorbent-based sampling methods for volatile and semi-volatile organic compounds in air. Part 2. Sorbent selection and other aspects of optimizing air monitoring methods, J. Chromatogr. A, 1217, 2685–2694, https://doi.org/10.1016/j.chroma.2010.01.015, 2010.

Yatavelli, R. L. N., Lopez-Hilfiker, F., Wargo, J. D., Kimmel, J. R., Cubison, M. J., Bertram, T. H., Jimenez, J. L., Gonin, M., Worsnop, D. R., and Thornton, J. A.: A Chemical Ionization High-Resolution Time-of-Flight Mass Spectrometer Coupled to a Micro Orifice Volatilization Impactor (MOVI-HRToF-CIMS) for Analysis of Gas and Particle-Phase Organic Species, Aerosol Science and Technology, 46, 1313–1327, https://doi.org/10.1080/02786826.2012.712236, 2012.

Zhou, W., Xu, W., Kim, H., Zhang, Q., Fu, P., Worsnop, D. R., and Sun, Y.: A review of aerosol chemistry in Asia: insights from aerosol mass spectrometer measurements, Environmental science. Processes & impacts, 22, 1616–1653, https://doi.org/10.1039/D0EM00212G, 2020.

Zhou, Y., Huang, X. H., Bian, Q., Griffith, S. M., Louie, P. K. K., and Yu, J. Z.: Sources and atmospheric processes impacting oxalate at a suburban coastal site in Hong Kong: Insights inferred from 1 year hourly measurements, J. Geophys. Res., 120, 9772–9788, https://doi.org/10.1002/2015JD023531, 2015.